Cancer Management and Research

Elevate Series

Open Access Full Text Article

ORIGINAL RESEARCH

Retinol Binding Protein 4 Serves as a Potential Tumor Biomarker and Promotes Malignant Behavior in Gastric Cancer

Yantao Yu[1–3,*], Chenkai Zhang[2,3,*], Qiannan Sun[2–4], Shantanu Baral[2,3], Jianyue Ding[2,3], Fanyu Zhao[2,3], Qing Yao[2,3], Shuyang Gao[2,3], Bin Liu[2–4], Daorong Wang[1–4]

[1]The Yangzhou School of Clinical Medicine of Dalian Medical University, Yangzhou, 225001, People's Republic of China; [2]General Surgery Institute of Yangzhou, Yangzhou University, Yangzhou, 225001, People's Republic of China; [3]Yangzhou Key Laboratory of Basic and Clinical Transformation of Digestive and Metabolic Diseases, Yangzhou, 225001, People's Republic of China; [4]Northern Jiangsu People's Hospital, Yangzhou, 225001, People's Republic of China

*These authors contributed equally to this work

Correspondence: Daorong Wang; Bin Liu, Email 18051062590@yzu.edu.cn; liubin2006cool@126.com

Background: Gastric cancer (GC) is a highly phenotypically heterogeneous disease and is caused by a combination of factors. Retinol binding protein 4 (RBP4) is a member of a family of lipid transport proteins that are involved in the transport of substances between cells and play a crucial role in a variety of cancers. However, the expression and role of RBP4 in GC remain unknown.

Methods: In this study, we explored the expression, prognostic significance, immune microenvironment, drug responsiveness and function of associated signaling pathways of RBP4 in GC using web-based bioinformatics tools. Immunohistochemistry and real-time quantitative PCR were utilized to analyze the tissue and cell expression levels of RBP4. CCK-8, colony formation, EDU incorporation, wound healing and transwell assays were applied to demonstrate the effect of RBP4 on GC cell function. Flow cytometric detection of apoptosis after RBP4 knockdown. Nude mice xenograft model elucidates the role of RBP4 for GC in vivo. Related proteins of the RAS signaling pathway were analyzed by employing Western blot assays.

Results: RBP4 is highly expressed in GC. RBP4 is closely associated with patient survival and sensitivity to a wide range of antitumor agents. Knockdown of RBP4 promoted apoptosis and inhibited cell proliferation, invasion and migration. RBP4 promotes GC tumorigenesis in vivo. Finally, RBP4 modulates the RAS/RAF/ERK axis.

Conclusion: RBP4 may promote gastric carcinogenesis and development through the RAS/RAF/ERK axis and is expected to be a novel target for GC treatment.

Keywords: RBP4, gastric cancer, invasion, migration, RAS/RAF/ERK axis

Introduction

Gastric cancer (GC) is a malignant tumor originating from the epithelium of the gastric mucosa and is currently the fifth most prevalent cancer globally. Statistics show that there are more than 1 million new cases of GC annually.[1] Geographic differences across the globe have contributed to the highest incidence rates in East Asia and Eastern Europe, while Northern Europe and North America generally have lower incidence rates.[2] Common risk factors for GC include Helicobacter pylori infection, genetics, smoking, and alcohol consumption. Besides, the incidence of GC is twice as high in males as in females.[3] Nowadays, the incidence of the disease in people aged <50 years is gradually increasing in both moderately dangerous and extremely dangerous countries.[4] Despite the frequent occurrence of GC, most patients are diagnosed at an advanced stage with a poor prognosis because there are no definite clinical symptoms, and the median survival for metastatic GC is less than 1 year.[5] In recent years, for patients with advanced GC, in addition to surgery and cytotoxic chemotherapy, molecularly targeted drugs are gradually becoming prevalent. For example, for HER-2-positive patients, common drugs include trastuzumab, lapatinib, and margetuximab, and these targeted therapies can improve survival and reduce toxicity.[5] As a result, the identifying of novel therapeutic targets for GC is of great significance in both diagnosis and treatment of patients with advanced GC.

Received: 29 May 2024
Accepted: 19 July 2024
Published: 24 July 2024

Retinol binding protein 4 (RBP4) belongs to the of the lipid transport protein family and the major transporter protein for vitamin A in the circulation.[6] RBP4 is secreted primarily by the liver and secondarily by adipose tissue. In normal human conditions, RA-bound RBP4 and thyroid transport protein (TTR) participate in human biological functions together as the holo-RBP4-TTR complex.[7] It has been shown that STRA6, as a cell surface receptor, can participate in bidirectional retinol transport thereby balancing RBP4 in the circulatory system with intracellular vitamin A metabolism and storage and counteracting vitamin A insufficiency or oversupply.[8] Changes of RBP4 levels in mice have been stated to be closely links to numerous diseases. For example, mice with a mixed genetic background lacking RBP4 revealed impaired retinal function and visual perception during the first few months, but subsequent feeding of retinol-containing food restored vision to normal by 4–5 months of age.[9] RBP4 mutations have been linked to osteoarthritis, and hypercholesterolemia and acne in people. Furthermore, RBP4 drives migration of ovarian cancer cells and exhibits high expression in hepatocellular carcinoma cells.[10,11] Nevertheless, there have been no correlation studies of RBP4 expression and potential mechanisms in GC.

The aim of this study was to investigate the expression of RBP4 in GC tissues and cells and its effect on the occurrence and progression in GC. We used small interfering RNA tools and lentiviral infection techniques to inhibit RBP4 levels in GC cells. On the one hand, in vitro experiments revealed that silencing of RBP4 inhibited the proliferation, invasion and migration of GC cells and promoted apoptosis. On the other hand, in vivo experiments further validated this biological process based on the size and weight of the mouse hormone tumors. At the final stage of the experiment, we explored the joint function of RBP4 and its closely associated signaling pathways for GC.

Materials and Methods

Bioinformatic Analysis

Data on gene expression profiles and clinical information were acquired from the TCGA database available at https://portal.gdc.cancer.gov. The expression of RBP4 was investigated across different cancer types, focusing on a GC cohort (STAD). Two groups, high and low expression levels, were compared using the "DESeq2" package. Gene set enrichment analysis (GSEA) was conducted based on logFC values. Survival analyses and exploration of RBP4 mutations were conducted utilizing the cBioPortal database (https://www.cbioportal.org/). Data on drug sensitivity were acquired from the CellMiner online repository (https://discover.nci.nih.gov/cellminer/home.do), followed by conducting a Pearson correlation analysis with RBP4. The Kaplan-Meier survival analysis was conducted based on the groupings obtained from the Kaplan-Meier plotter tool available at https://kmplot.com/analysis/. Protein-protein interaction analysis for RBP4 was performed using the String database (https://string-db.org/).

Patients and GC Specimens

We gathered 80 pairs of formalin-fixed and paraffin-embedded human GC specimens, ages 50 to 80, between January 2023 and January 2024. The specimens used in this study were provided by the Northern Jiangsu People's Hospital. Notably, neither of the patients had chemotherapy prior to surgery. This project has been approved by the Ethics Committee (Yangzhou, China), Yangzhou University School of clinical Medicine, and Northern Jiangsu People's Hospital. Permission number 2019KY-022. Written informed consent was provided by each participant before to the trial. This study was conducted in accordance with the principles set out in the Declaration of Helsinki.

Immunohistochemistry (IHC)

The tissue sections of TMA were placed in an oven at 65°C for a duration of 2 hours. Following this, they were allowed to cool to room temperature and then deparaffinized using a mixture of xylene and ethanol in a range of 100% to 50%. Antigen repair was performed using sodium citrate (Solarbio, Beijing, China) for 20 minutes, and endogenous peroxidase activity was blocked using 5% H_2O_2. After closure with drops of goat serum for 20 minutes (OriGene, Jiangsu, China), the primary antibody RBP4 (1:50, Proteintech, China) was added overnight at 4°C in the refrigerator. On the following day, a rabbit secondary antibody (OriGene, Jiangsu, China) was added dropwise and incubated for 25 minutes at 37°C in an incubator. After three rinses with phosphate buffered saline (PBS), staining was performed for 5 minutes

using DAB chromogenic solution (OriGene, Jiangsu, China), followed by a reaction using hematoxylin (Beyotime, Shanghai, China) for 3 minutes. After sealing the slices with resin, TMA tissues were observed and photographed using an Olympus microscope. The obtained images are scored on the following scale: Scoring for staining was as follows: Absence of staining = 0, weak-to-strong complete nuclear staining in less than 25% of tumor cells = 1, weak-to-strong complete nuclear staining in 25% to 50% of tumor cells = 2, strong complete nuclear staining in 50% or more of tumor cells = 3. Expression levels were categorized as low (scores 0 and 1) or high (scores 2 and 3).[12] The results were independently scored by two excellent pathologists.

Cell Lines and Cell Culture

The Bank of the Chinese Academy of Sciences provided us with 4 GC cell lines (AGS, N87, HGC-27 and BGC-823) as well as the normal human stomach cell lines (GES1). The cell lines were cultured in RPMI1640 medium (Eallbio, Beijing, China),37°C (5%CO_2) incubator. For better cell growth, we added 10% fetal bovine serum (Solarbio, Beijing, China), 1% penicillin and streptomycin (Vazyme, Nanjing, China). No signs of mycoplasma or fungal contamination were found during the experiment.

Western Blot

Tissues and cells were lysed on ice using RIPA lysis solution (Solarbio, Beijing, China). The lysate from the reaction was collected by centrifugation at 14,000 rpm at 4°C for ten minutes. The protein lysates' absorbance values at 570 nm were determined using a BCA kit (Yeasen, Shanghai, China). The absorbance of each sample was counted to make a protein standard curve. It was mixed with an appropriate amount of 5X Loading buffer and boiled for 7 minutes. Subsequently, the samples were electrophoresis on an SDS-PAGE gel for 2 hours and transferred to a PVDF membrane (Immobilon-P, Merck Millipore, Ireland). After closure utilizing 5% skimmed milk, the first antibody was incubated at 4°C for the whole night. The investigation employed the following antibodies: RBP4 (1:800, Proteintech), GAPDH Rabbit mAb (1:8000, Abclonal), E-cadherin (1:800, Affinity), N-cadherin (1:700, Affinity), MMP2 (1:800, Affinity), MMP3 (1:800, Affinity), MMP9 (1:800, Affinity), P53 (1:700, ZEBIO), BAX (1:1000, ZEBIO), BCL2 (1:1000, ZEBIO), Caspase3 (1:800, Proteintech), Cleaved-Caspase3 (1:700, Proteintech), Caspase9 (1:600, Proteintech), Cleaved-Caspase9 (1:600, Proteintech), RAS (1:600, Proteintech), RAF (1:600, Proteintech), ERK (1:600, Proteintech). On the next day, the PVDF membrane was placed in Goat anti-Rabbit IgG (1:7000, Abclonal) and Goat anti-Mouse IgG (1:7000, Abclonal) after 1 hour incubation at room temperature, developed using ECL reagent (Vazyme, Nanjing, China). Data were analyzed using ImageJ and the experiment was repeated three times.

Real-Time Quantitative PCR (RT-qPCR) Assays

The RNA was isolated from the cell lines by employing Trizol reagent (Yeasen, Shanghai, China) and then transformed into cDNA through the utilization of a reverse transcription kit (Yeasen, Shanghai, China), followed by RT-qPCR conducted with a SYBR Green PCR kit (Vazyme, Nanjing, China). The amplification program for this experiment used a two-step method with the following settings: 95°C for 5 minutes, 5 seconds at 95°C, 30 seconds at 60°C, and a total of 40 cycles. The primers were provided by Gene Pharma, Suzhou, China, and the specific sequences are as follows:RBP4-forward (5′-AGGAGAACTTCGACAAGGCTC-3′), RBP4-reverse (5′-GAGAACTCCGCGACGATGTT-3′), GAPDH forward (5′-TGACATCAAGAAGGTGGTGAAGCAG-3′), GAPDH reverse (5′-GTGTCGCTGTTGAAGTCAGAG GAG-3′). The relative expression of experimental cells was determined using the $2^{-\Delta\Delta Ct}$ method, with GAPDH serving as the internal reference.

Transient Transfection and Lentivirus Infection

GenePharma (Shanghai, China) prepared the small interfering RBP4 (si-RBP4) and negative control (NC). The following are the sequences: NC-forward (5′-UUCUCCGAACGUGUCACGUTT-3′), NC-reverse (5′-ACGUGACACGUUCGGAGAATT -3′), si1-RBP4-forward (5′-GCUUCCGAGUCAAGGAGAATT-3′), si1-RBP4-reverse (5′-UUCUCCUUGACUCGGAAG CTT-3′), si2-RBP4-forward (5′-GCACCUGUGCUGACAGCUATT-3′), si2-RBP4-reverse (5′-UAGCUGUCAGCACAGGU GCTT-3′). The RBP4-silencing lentivirus (shRBP4) was constructed by Genechem (Shanghai, China). The specific sequence

is as follows: shRBP4 (5′-CTCAGTCTTCAGCTCTATTTA-3′). In 6-well plates, 2×10^5 GC cells were seeded and allowed for growth for a whole night. On the following day, a mixture of small interfering RNA and lipofectamine 2000 (Invitrogen, USA) was transfected into GC cells, and transient transfection was completed. GC cells were infected with lentivirus for 72 hour and then uninfected GC cells were removed by adding 2μg/mL of Puro-mycin to the culture medium, and the stably RBP4 knockdown cell lines was successfully constructed.

Cell Counting Kit-8 (CCK-8) Assay

Cells were cultured in a 96-well plate with 1000 cells per well, and the medium was removed using a pipette gun at 24, 48, 72, and 96 hours after incubation. The CCK-8 reagent (MedChemExpress, USA) was prepared and added to the cells. To generate a standard curve, the cells' absorbance value at 450 nm was measured with a microplate reader.

Colony Formation Assay

In a 6-well plate, 500 GC cells that have been transfected and infected were added. Following two weeks of cultivation in a 37°C (5%CO_2) cell incubator, the cells had three PBS washes, were fixed with 4% paraformaldehyde and were stained for 7 minutes with 5% crystal violet solution. Data statistics were performed using ImageJ.

EDU Incorporation Assay

The experimental cells were placed into 6-well plates and treated with EDU reagent (Invitrogen) after 48 hours. The cells were then permeabilized for 8 minutes using 0.5% TritonX-100 and fixed with 4% paraformaldehyde. Utilizing a Click-iT EDU Assay kit (Invitrogen), EDU incorporation was identified. Using a fluorescence microscope, the images of cells in five distinct viewpoints were captured and subsequently analyzed with Image-Pro Plus software. Cells that were positive for DAPI were tallied as the overall cell count, while cells stained with EDU were tallied as EDU-positive cells.

Wound Healing Assay

The cells were inoculated in Petri dishes and cultured in serum-free RPMI-1640 medium. When the cell density reached 90% or more, the cell monolayer was scraped perpendicular to the petri dish with a lance tip of 200μL volume, and the cell debris was washed with PBS. Cell migration was observed and recorded at 0 and 24th hour using an Olympus microscope, and each photograph was taken in an independent field of view.

Transwell Migration and Invasion Assays

In migration experiments, 200μL of serum-free RPMI-1640 cell mixture (number of cells:2×10^4) was added to the upper section of every chamber (Coring, USA) and 500μL of serum-containing RPMI-1640 medium was filled into the lower layer of the chamber. In the invasion experiment, 50μL of diluted artificial matrix gel (BD Biosciences, USA) was spread in the upper chamber one night in advance, and when the matrix gel solidified, 200μL of RPMI-1640 cell mixture was filled into the upper chamber, while 500μL of FBS-containing medium was added into the lower chamber. After 48 hours, cells were immobilized using 4% paraformaldehyde, dyed with 1% crystal violet for a duration of 15 minutes, then captured in five different areas through light microscopy. The data was subsequently processed and analyzed for statistical significance with the assistance of ImageJ software.

Flow Cytometry

GC cells were collected by centrifugation (1000r/min, 5 min) after treatment with trypsin, and the cells were processed according to the instructions of the apoptosis detection kit (Aladdin Biochemical, Shanghai, China). After three washes with PBS, 500μL of pre-cooled PBS was added, followed by 15μL of AnnexinV-fluorescein isothiocyanate (FITC) and 7μL of propidium iodide (PI). Following a 30-minute incubation at 4°C in the absence of light, the examination was carried out utilizing flow cytometry.

Tumor Xenograft Model

Randomly, the adult nude mice (JiBiological, Nanjing, China) were divided into four groups (A, B, C, D) with three mice in each group. AGS cells (shRBP4) that had been infected with lentivirus were injected into B. Similarly, HGC-27 cells (shRBP4) that had been infected with lentivirus were injected into D to construct a mice subcutaneous tumor xenograft model. A and C are blank control groups. Tumor volumes in mice were measured on a weekly basis and computed using the formula V= (Length×Width^2)/2. After four weeks, every mouse was euthanized, and the xenograft tumors were removed and weighed. Experiments involving animals are authorized by the Ethics Committee for Experimental Animals at Yangzhou University and carried out in compliance with the National Institutions of Health Guidelines for the Care and Use of Laboratory Animals.

Statistical Analysis

Experimental data were analyzed statistically with GraphPad Prism 9 (SanDigeo, CA, USA). The student's test was used to compare differences between the two groups, and one-way ANOVA was employed for analyzing three or more groups. Statistical significance was determined using the following criteria: *P<0.05, **P<0.01, ***P<0.001, ****P<0.0001.

Results

Genetic Alterations and Mutational Landscapes of RBP4

Examining RBP4's relative expression in 26 different types of cancer revealed high expression in GC (Figure 1A). Analysis on cBioPortal revealed an overall mutation rate of RBP4 at 1%, with GC (STAD) exceeding the average and ranking 9th (Figure 1B). Furthermore, we explored the mutation sites and types of RBP4, identifying nonsense mutations, splice mutations, truncating mutations, amplifications, and deep deletions (Figure 1C). Notably, deep deletions represented the majority of mutations (Figure 1D). Survival analysis indicated that high RBP4 gene mutations were associated with a negative impact on overall survival across various cancers (21.51 vs 50.63 months, P=0.003845) (Figure 1E).

Relationship Between RBP4 Expression and Tumor Immune Infiltration, Drug Sensitivity Analysis

Using the TISIDB database, we investigated the potential impact of RBP4 on tumor immune infiltration and its relationship with current immunological agents. Our findings suggest that RBP4 negatively regulates common immune cells in GC, showing a weak but very limited association with certain immune stimulants and inhibitors (Figure 2A). Furthermore, the weaker immune infiltration of RBP4 in GC seems to correlate with targeted drugs. To identify potential drug targets, we utilized the Cellminer database. Our analysis demonstrated a positive association between RBP4 and caffeic acid (R=0.4; P=0.001) as well as Kahalide F (R=0.36; P=0.007), while BP-1-102 (R=−0.36; P=0.005) and LY-2606368 (R=−0.38; P=0.003) were negatively associated with RBP4 (Figure 2B). These results provide valuable insights for tailoring treatment regimens for patients exhibiting high RBP4 expression.

RBP4 Expression Was Upregulated in GC and Correlated with Patient Survival

We produced volcano plots through the DEGs of the STAD cohort showing that RBP4 is located in the highly expressed fraction (Figure 3A). Furthermore, the boxplot revealed that RBP4 was highly expressed in GC (Figure 3B). GC patients with higher RBP4 expression have significantly poorer survival rates according to Kaplan Meier-plotter database (Figure 3C and D). Therefore, in order to validate the expression of RBP4 in GC, we used IHC and Western blot experiments on tissues to verify that RBP4 was markedly upregulated in GC tissues (Figure 4A and B). In addition to validation at the tissue scale, we also analyzed at the cellular scale. Using RT-qPCR, we learned that the mRNA expression of RBP4 was significantly higher in GC cells than in normal cells (Figure 4C), and since the results of the Western blot experiments on cell lines were basically the same as those of RT-qPCR (Figure 4D), we chose AGS and HGC-27 cells, which had relatively high expression of RBP4, for the knockdown experiments in cells. Knockdown of RBP4 in both groups of cells using small interfering RNA technology found that both si1-RBP4 and si2-RBP4 were

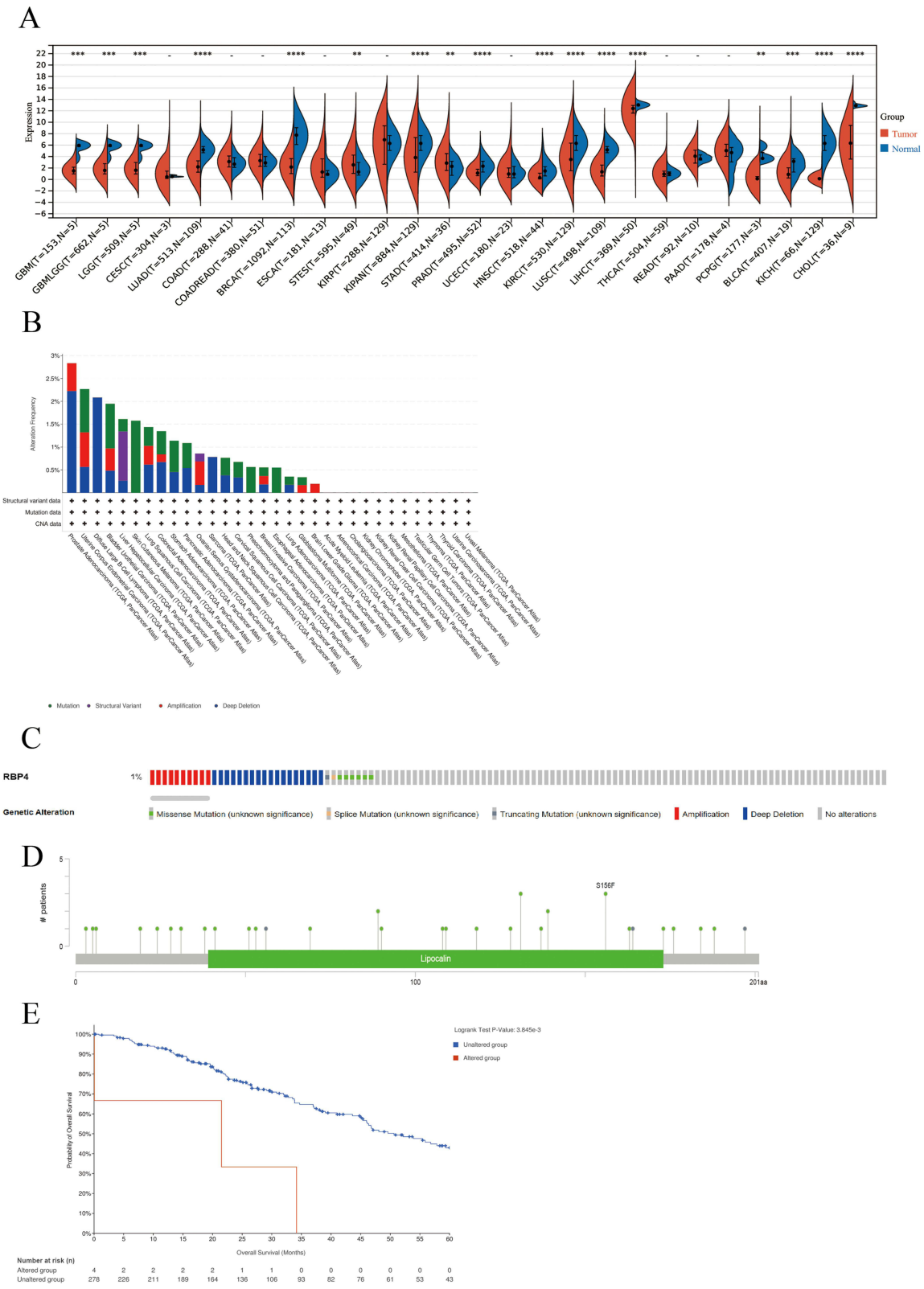

Figure 1 Genetic alterations and mutational landscapes of RBP4. (**A**) Relative expression of RBP4 in 26 different types of cancers. (**B**) Distribution of RBP4 mutations across various cancer types. (**C**) Comprehensive overview of RBP4 mutations in pan-cancer. (**D**) Mutation sites identified within the RBP4. (**E**) Survival analysis of alterations in RBP4. ***P*<0.01, ****P*<0.001, *****P*<0.0001.

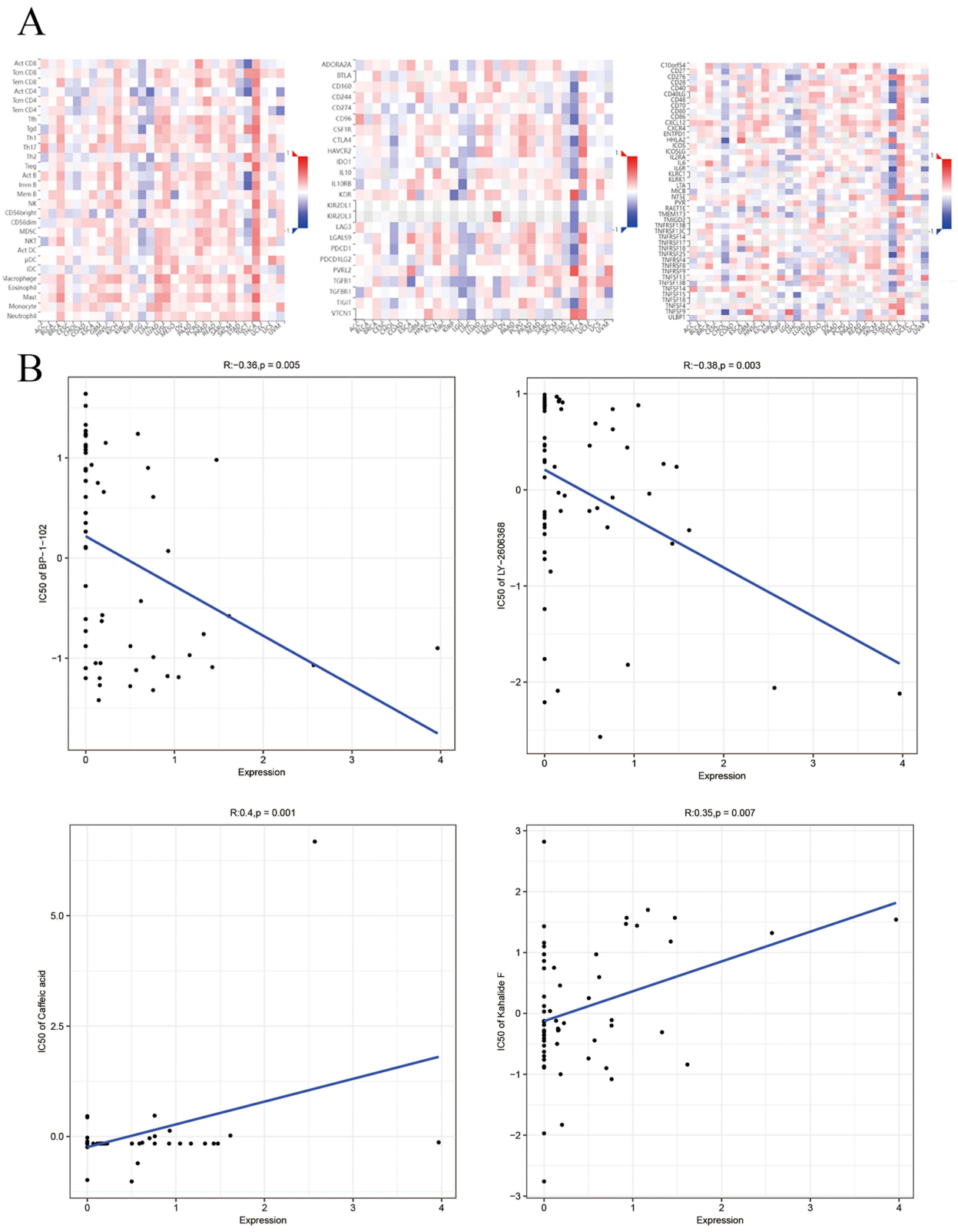

Figure 2 Relationship between RBP4 expression and tumor immune infiltration, drug sensitivity analysis. (**A**) Relationship between RBP4 and multiple tumor immune infiltration, immune stimulants/inhibitors. (**B**) The association between RBP4 expression and drug sensitivity.

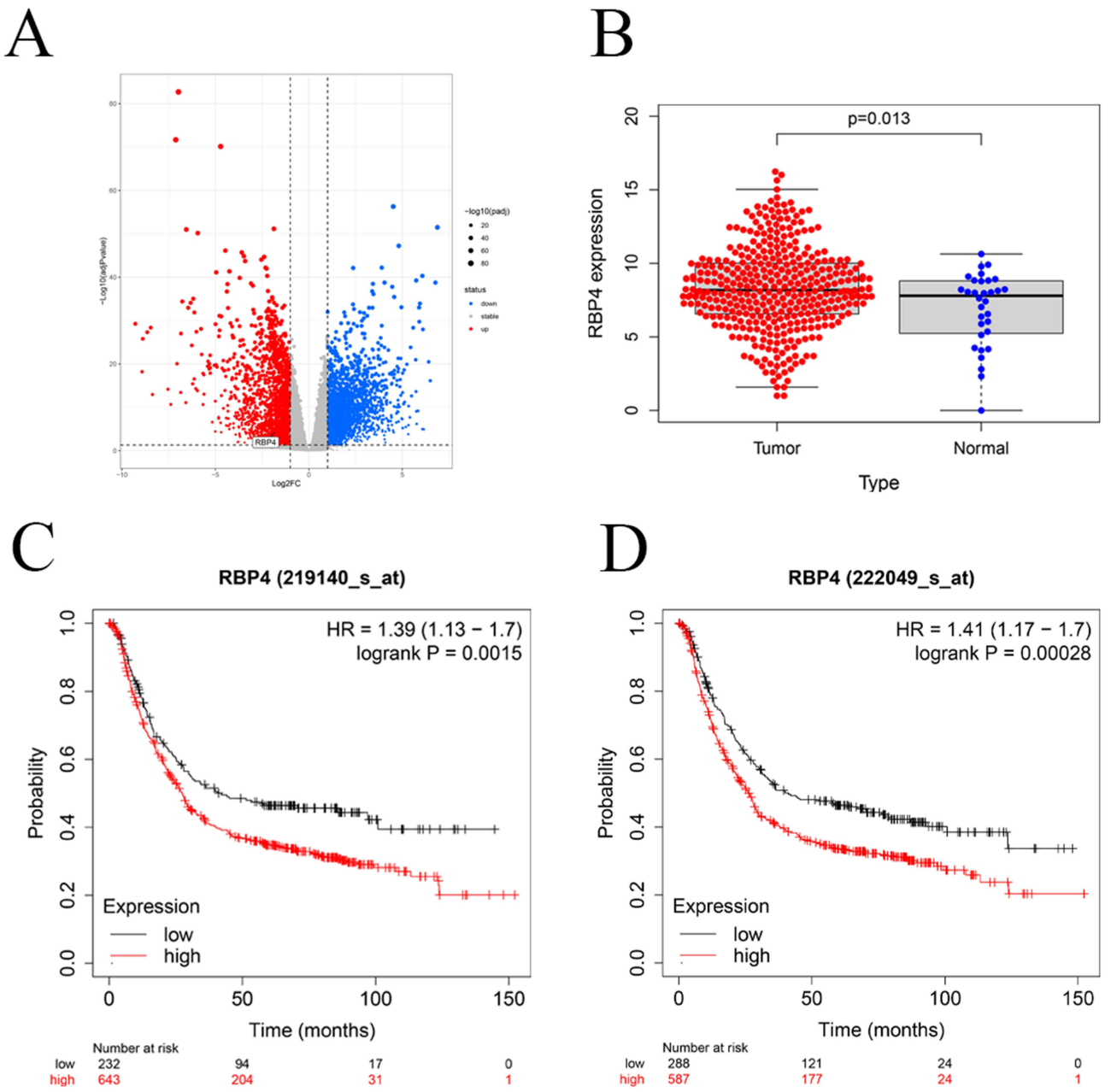

Figure 3 RBP4 showed high expression in GC analyzed by online database. (**A**) The Volcano map showed all differentially expressed genes. (**B**) RBP4 expression in tumor tissues and normal tissues was analyzed using the TCGA database. (**C** and **D**) Kaplan–Meier plotter database indicated that GC patients with high RBP4 expression had a poor prognosis (two probes: probe ids: 219140_s_at and 222049_s_at).

statistically significant compared to the NC group (Figure 4E), so both small interferences will be used together as a follow-up experiment.

Knockdown of RBP4 Inhibits Proliferation, Migration and Invasion in GC Cells

The CCK-8 assay is an important criterion for testing the cell proliferation ability. In AGS cells, the proliferation ability of the experimental group was found to be markedly reduced at 48, 72 and 96 hours (Figure 5A), and in HGC-27 cells, it was found that the absorbance values at 450 nm were statistically significant in the si1-RBP4 and si2-RBP4 groups compared to NC group after 48 hours (Figure 5B). Using colony formation assays, it was demonstrated that the colony formation ability of the knockdown group was markedly reduced in both AGS and HGC-27 cells compared to the

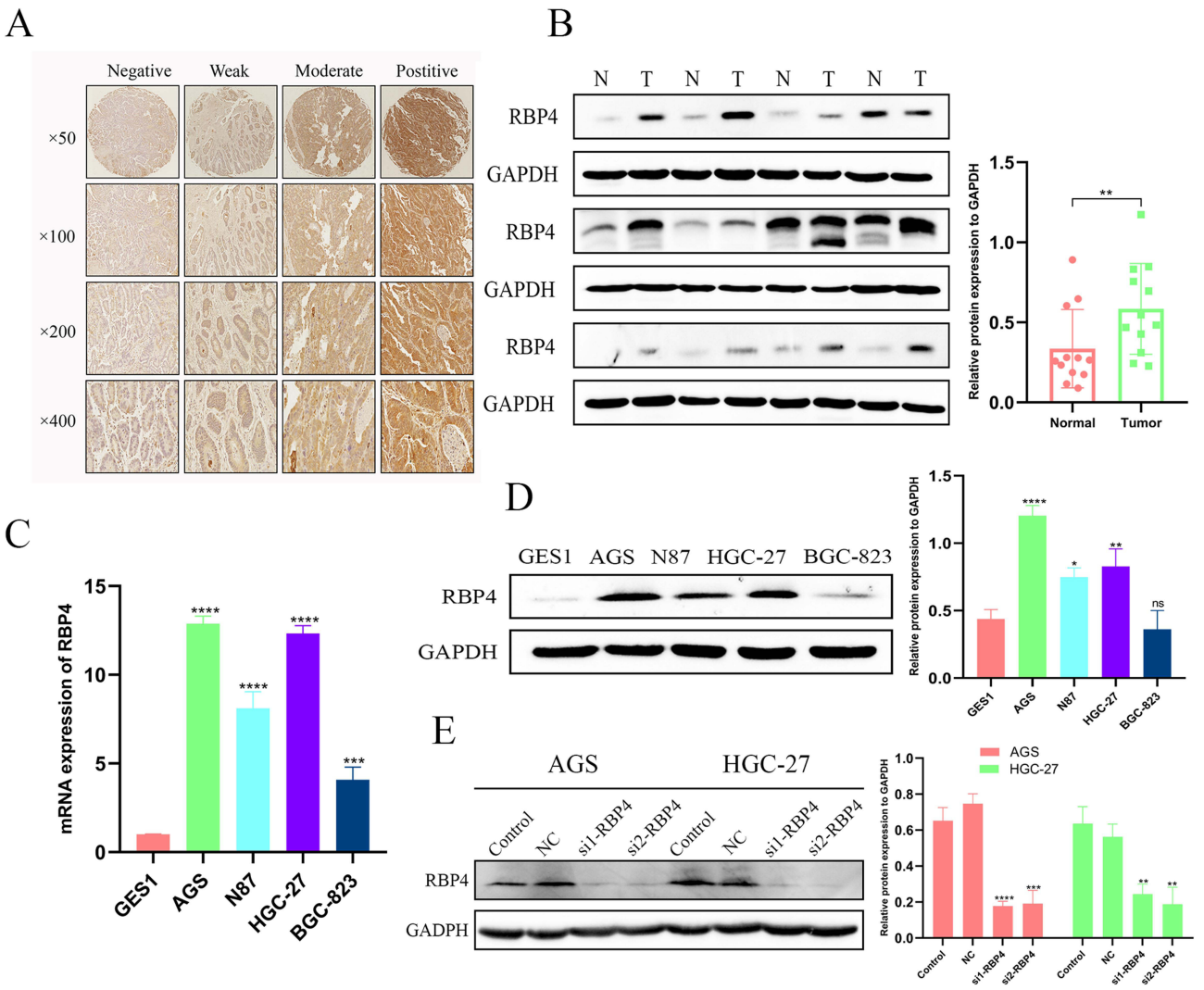

Figure 4 RBP4 expression is upregulated in GC tissues and cells. (**A**) Immunohistochemistry was performed on 80 pairs of GC specimens and showed representative images of RBP4 staining. (**B**) 12 pairs of tissues were randomly selected from 80 pairs of specimens to verify the expression level of RBP4 by Western blotting experiments and the associated grey value analysis of its results (N: Normal, (**T**) Tumor). GAPDH as a reference. (**C**) RBP4 mRNA expression levels in normal gastric cell (GES1) and GC cells (AGS, N87, HGC-27, BGC-823). (**D**) Protein levels of RBP4 in normal stomach cells and GC cells. (**E**) Silencing of RBP4 protein expression levels in AGS and HGC-27 cells (Control: blank control, NC: Negative Control, si1-RBP4: The first small interference, si2-RBP4: The Second small interference). ns: not significant. *P<0.05, **P<0.01, ***P<0.001, ****P<0.0001.

Control cells (Figure 5C). Moreover, we found that the EDU positive rate of cells knocking down RBP4 in AGS and HGC-27 cells was significantly different from that of Control cells by using EDU incorporation experiments (Figure 5D). The above experiments validated that silencing of RBP4 inhibited the proliferation ability of GC cells. To understand better the other biological functions of RBP4 in GC cells, we know that the migration ability of AGS and HGC-27 cells knocked down by RBP4 was significantly reduced after 24 hours compared with that of non-knocked down RBP4 cells by wound healing assay (Figure 6A). Besides, we demonstrated that the migration and invasion abilities of AGS and HGC-27 cells were markedly decreased when knocking down RBP4 by using Transwell assay (Figure 6B). Epithelial mesenchymal transition (EMT) is an important biological behavior that confirms invasion and migration capabilities.[13] Therefore, we demonstrated that in AGS cells, the levels of N-cadherin, MMP2, MMP3, and MMP9 decreased to various degrees after knockdown of RBP4, whereas the level of E-cadherin was obviously increased, by using Western blot assay (Figure 6C). In HGC-27 cells, knockdown of RBP4 cells showed a significantly decreased level of N-cadherin, MMP2, and MMP9, however, there was no noticeable variance in MMP3, and the level of E-cadherin was markedly increased (Figure 6C). In summary, knockdown of RBP4 suppressed the proliferation, migration and invasion in GC cells.

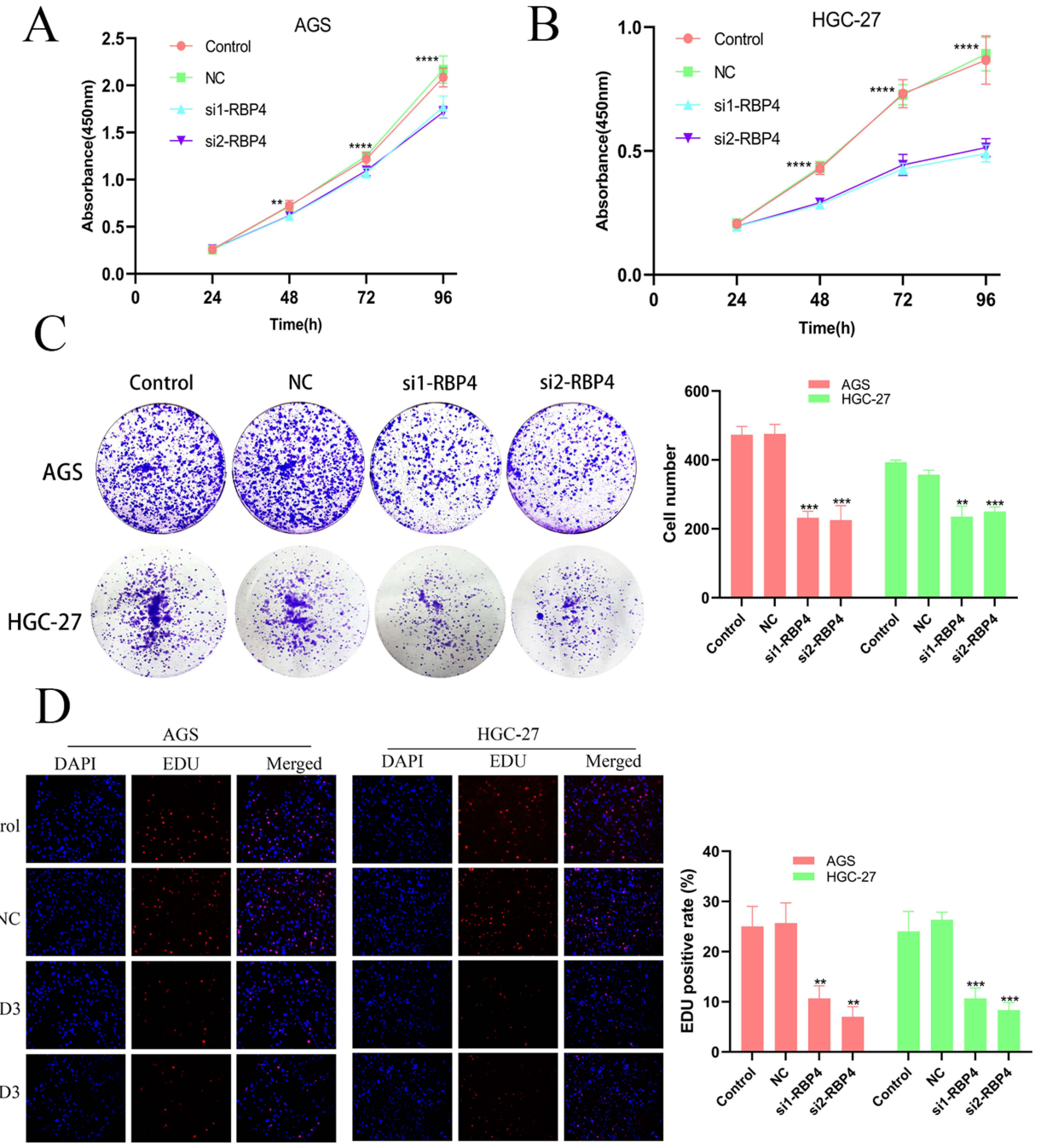

Figure 5 Knockdown of RBP4 inhibited the proliferation of GC cells. (**A**) In AGS cells, after silencing RBP4 by si-RNA1 and si-RNA2, the proliferation ability of the cells was detected using the CCK-8 assay. (**B**) The changes in cell proliferation ability after knockdown of RBP4 in HGC-27 cells. (**C**) The colony formation assay demonstrates a reduction in the ability to form colonies following the suppression of RBP4 in AGS and HGC-27 cell lines. (**D**) EDU incorporation assay revealed that silencing of RBP4 suppressed the proliferation ability of AGS and HGC-27 cells. ***P*<0.01, ****P*<0.001, *****P*<0.0001.

Knockdown of RBP4 Promotes Apoptosis in GC Cells

As knockdown of RBP4 inhibited the proliferation ability of GC cells, we verified whether RBP4 was associated with apoptosis. It was revealed by flow cytometry that the apoptosis capacity of cells in both the si1-RBP4 and si2-RBP4 groups in AGS and HGC-27 cells was significantly increased in comparison to the NC group (Figure 7A). Therefore, we utilized Western blot assay to analysis whether GC cells knocking down RBP4 are closely associated with relevant apoptosis molecules. The results (Figure 7B) of the experiments showed that in AGS cells, the levels of P53, BAX, Cleaved-Caspase3, and Cleaved-Caspase7 were markedly elevated in the cells after knockdown of RBP4, whereas the

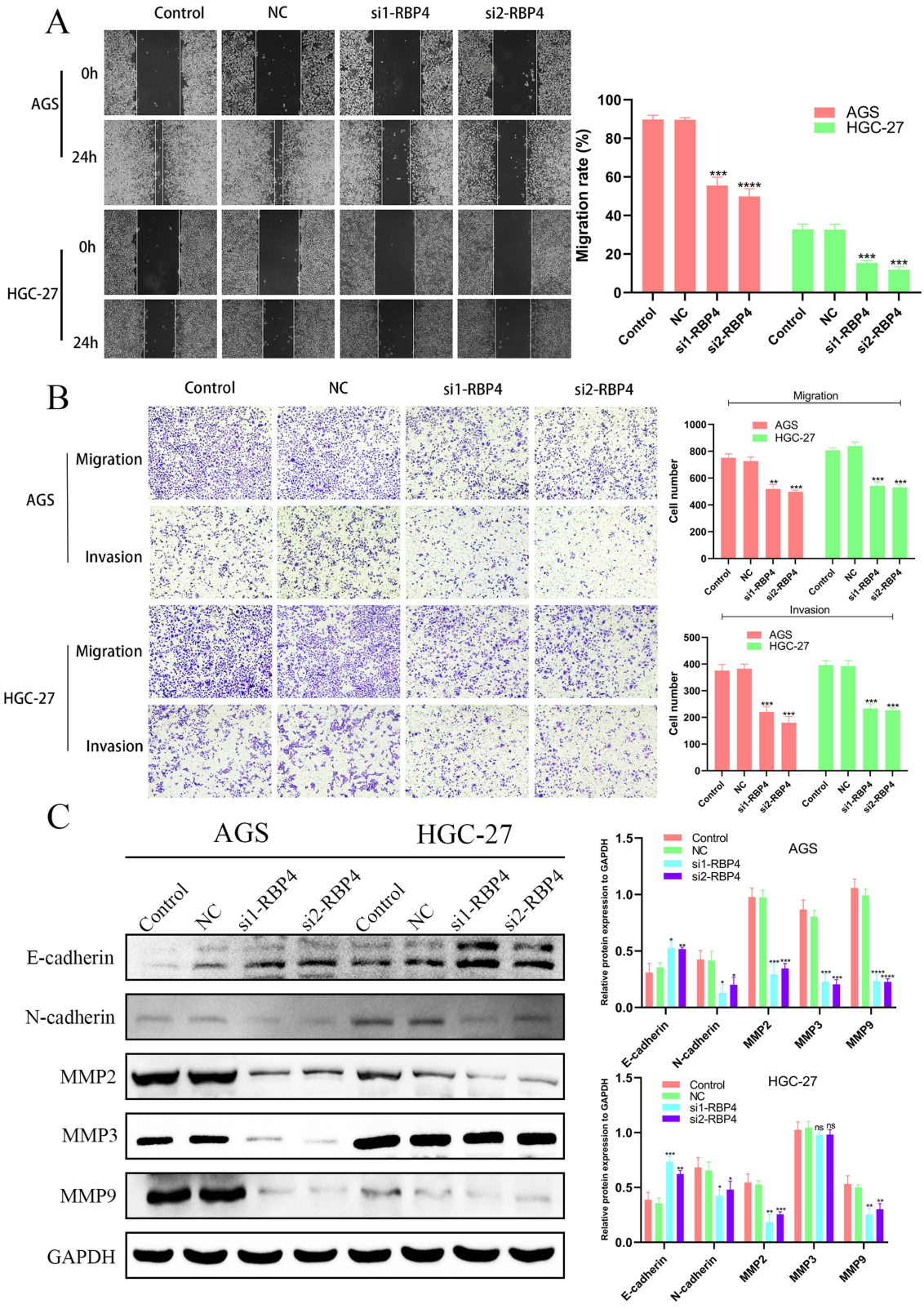

Figure 6 Knockdown of RBP4 inhibited the migration and invasion ability of GC cells. (**A**) Confirmation of migration ability of AGS and HGC-27 cells by wound healing assay. (**B**) Knockdown of RBP4 in AGS and HGC-27 cells was demonstrated to inhibit the migratory and invasive ability of GC cells using transwell assay. (**C**) The protein levels of E-cadherin, N-cadherin, MMP2, MMP3, and MMP9 were analyzed through Western blot experiments following the knockdown of RBP4 in AGS and HGC-27 cells. ns: not significant. **P*<0.05, ***P*<0.01, ****P*<0.001, *****P*<0.0001.

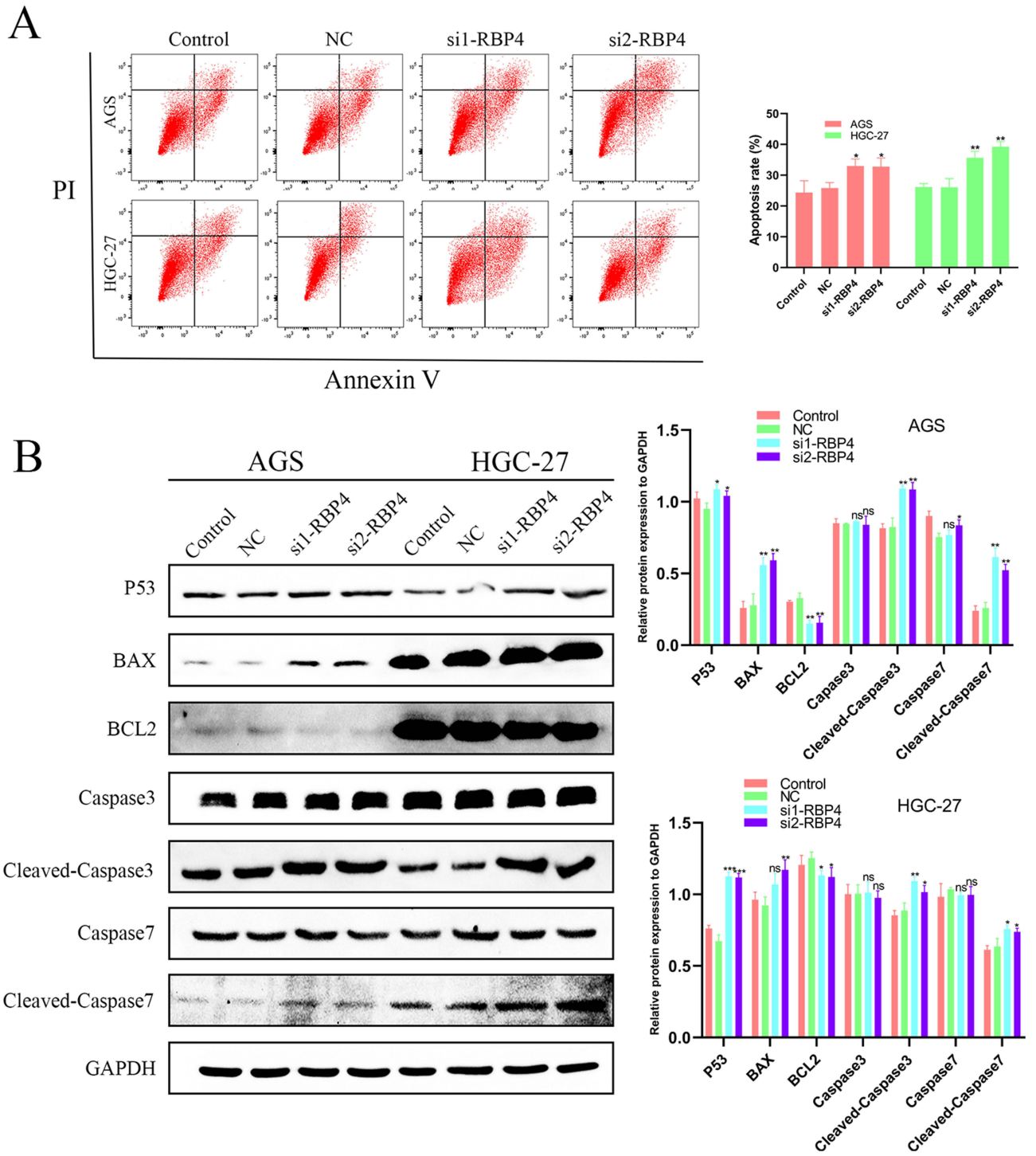

Figure 7 Silencing of RBP4 inhibits apoptosis in GC cells. (**A**) The effect of RBP4 knockdown on apoptosis in AGS and HGC-27 cells was tested by flow Cytometry. (**B**) Western blot analysis of the expressions of P53, BAX, BCL2, cleaved-caspase3/caspase3, cleaved-caspase7/caspase7, in Control cells, NC cells, and RBP4-knockdown cells of AGS and HGC-27 cell lines. ns: not significant. *P<0.05, **P<0.01, ***P<0.001.

level of BCL2 was significantly reduced, and there was no obvious change in the levels of Caspase3 and Caspase7. In HGC-27 cells, P53, Cleaved-Caspase3 and Cleaved-Caspase7 were significantly elevated and BCL2 levels were decreased and no obvious fluctuation of BAX, Caspase3 and Caspase7 was observed for si1-RBP4 group. In the si2-RBP4 group, P53, BAX, Cleaved-Caspase3, and Cleaved-Caspase7 were markedly increased, however, BCL2 levels

were decreased, and there were no obvious changes in Caspase3 and Caspase7. The above experiments show that RBP4 is involved in regulation of apoptosis process.

Knockdown of RBP4 Inhibited the Growth of GC Cells in vivo

In vitro experiments basically explained the role of RBP4 in GC progression, nevertheless, in vivo experiments are essential to verify the involvement of RBP4 in the process of GC occurrence. In this study, we established a GC xenograft tumor model in mice by injecting AGS and HGC-27 cells expressing shRBP4 lentivirus infection into mice, and we divided them into four groups (A=AGS-Control, B=AGS-shRBP4, C=HGC-27-Control, D=HGC-27-shRBP4) (Figure 8A–D). Among groups A and B, we measured the subcutaneous tumor volume of mice weekly and found that the tumor volume of group B mice injected with AGS cells after weeks 3 and 4 was markedly lower than that of group A mice without any treatment (Figure 8B). Tumors were removed from the mice at week 4 of execution to measure the weights and it was found that the weights in the shRBP4 group were statistically lower than those in the Control group (Figure 8C). Similarly, the results of groups C, D demonstrated that the volume and weight of tumors in group D mice injected with HGC-27 cells were significantly different from those in untreated group C (Figure 8E and F). The above results indicated that knockdown of RBP4 inhibited the growth of GC cells in mice.

RBP4 Knockdown Inhibits GC Growth by Regulating Inactivation of the RAS/RAF/ERK Axis

Because of the complexity of cancer, its malignant behavior is often the result of multiple sets of microscopic molecules working together. Initially we used the String database to find the top ten most relevant genes for RBP4 (Figure 9A).

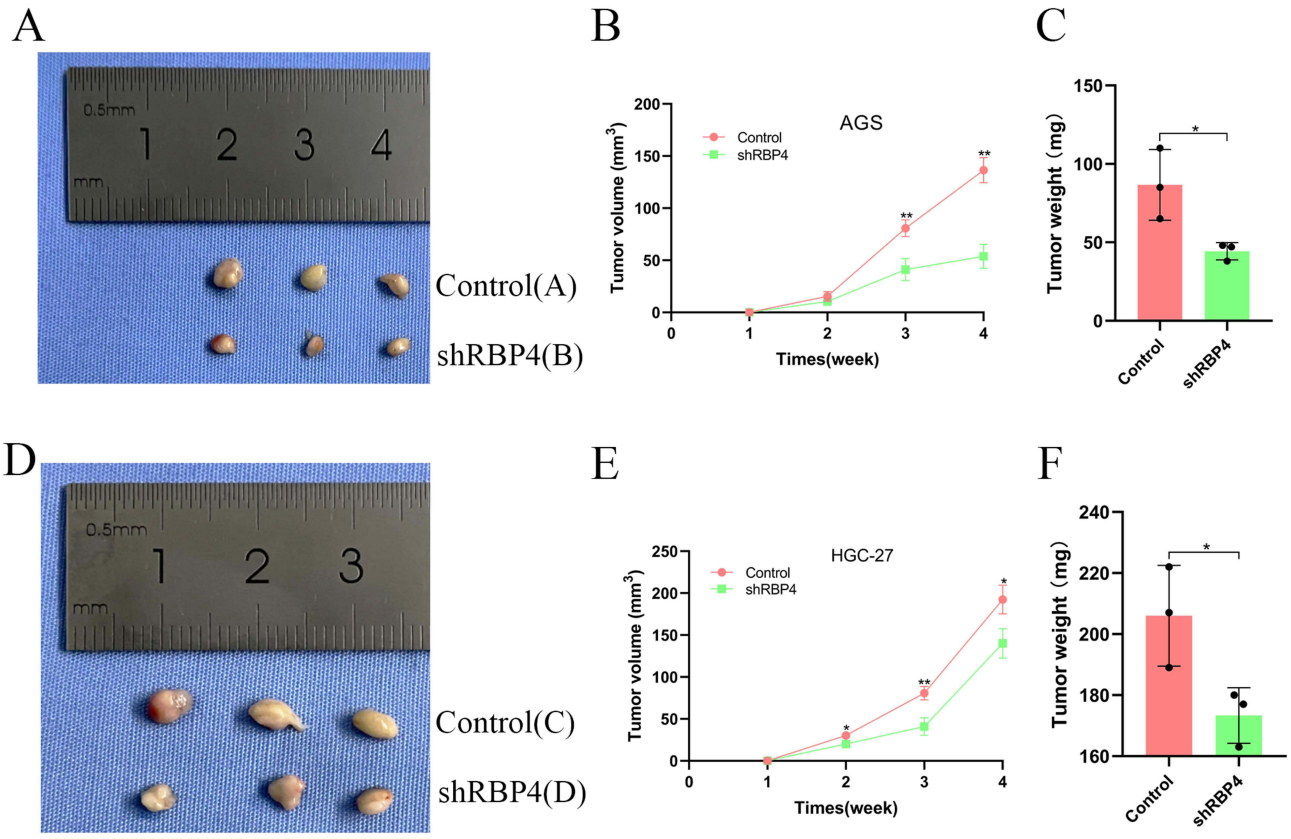

Figure 8 RBP4 promotes tumorigenesis in vivo. (**A**) The mice xenograft tumor model was established by injecting AGS cells that had been infected with RBP4 lentivirus into the mice. (**B**) Tumor volume in mice within 4 weeks. (**C**) Tumor weight after resection. (**D**) The mice xenograft tumor model was established by injecting HGC-27 cells already infected with RBP4 lentivirus into the mice. (**E**) Tumor volume. (**F**): Tumor weight (Control (**A**) No cells injected, shRBP4 (**B**) Injection of RBP4 lentivirus-infected AGS cells, Control (**C**) No cells injected, ShRBP4 (**D**) Injection of RBP4 lentivirus-infected HGC-27 cells). *P<0.05, **P<0.01.

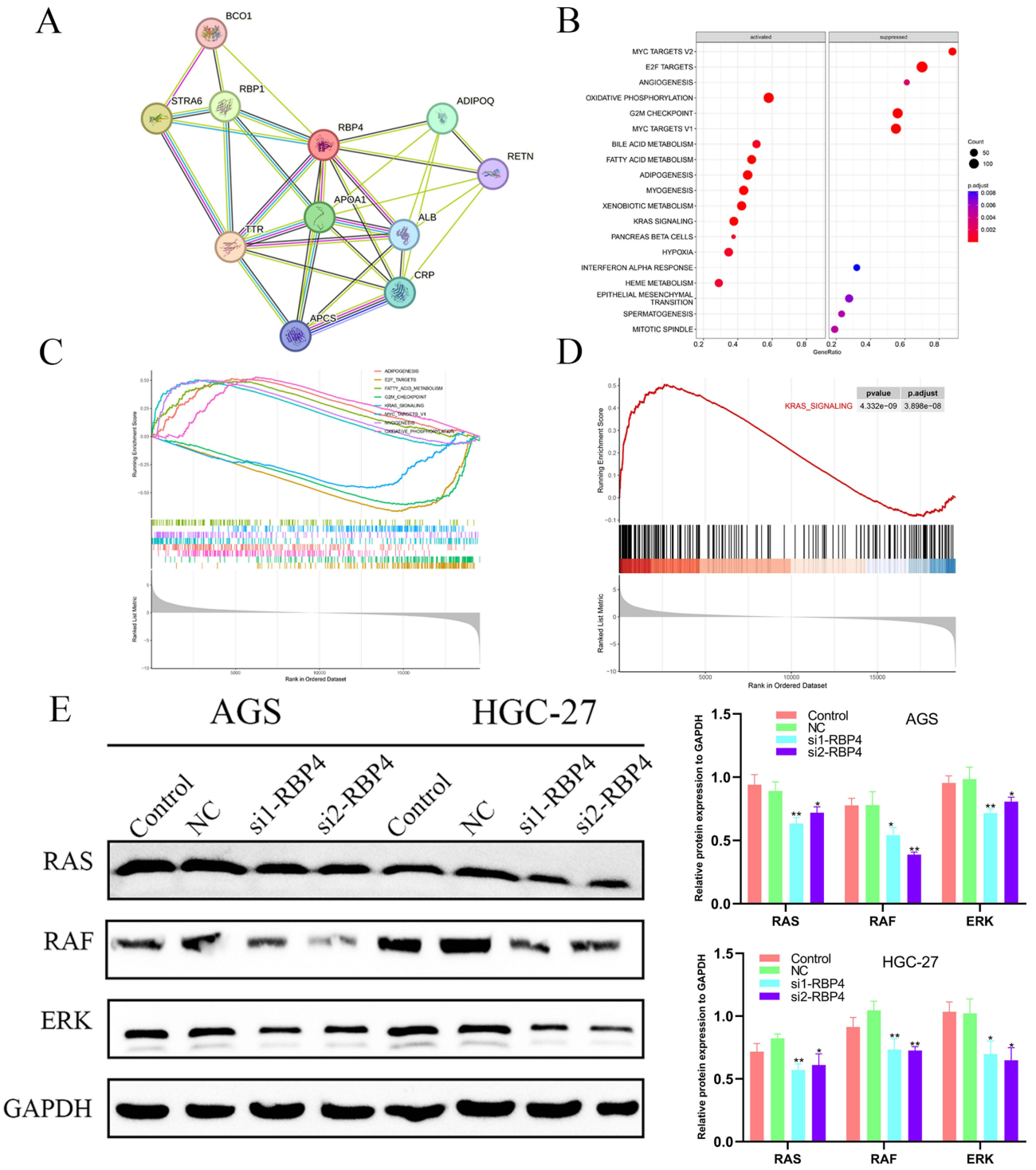

Figure 9 RBP4 regulates the RAS/RAF/ERK axis. (**A**) RBP4-related proteins were analyzed using the String tool. (**B** and **C**) Pathways enriched to GSEA based on RBP4 expression. (**D**) RBP4 high expression group for KRAS pathway modulation. (**E**) Variation of RAS, RAF and ERK protein levels in Control, NC, si1-RBP4 and si2-RBP4 groups after knockdown of RBP4 in AGS and HGC-27 cells. *P<0.05, **P<0.01.

Next, based on the median expression, we categorized the STAD cohort into one high levels of expression and one with low level of expression. After GSEA analysis, we found that RBP4 could potentially play a role in the modulation of numerous common pathways associated with cancer (Figure 9B and C), which were shown to be closely related to the RAS signaling pathway by differential analysis (Figure 9D). To verify this hypothesis, we observed a significant decrease

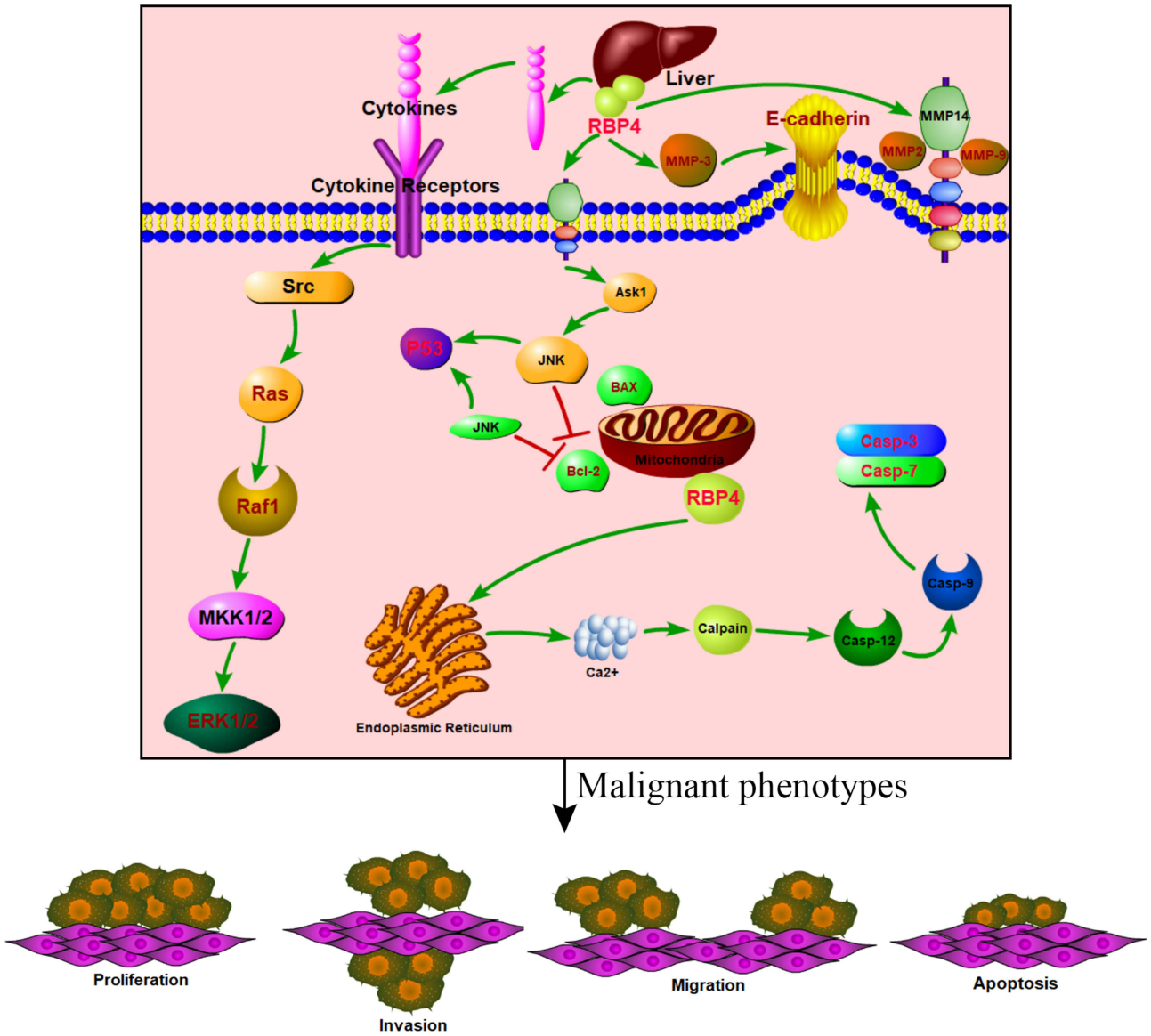

Figure 10 Diagram illustrating the molecular mechanism of RBP4 involvement in related pathways.

in the levels of RAS, RAF, and ERK proteins in AGS cells following the knockdown of RBP4 (Figure 9E). Similarly, in HGC-27 cells, the expression of RAS, RAF, and ERK showed a marked decrease in si1-RBP4 and si2-RBP4 than in the NC group (Figure 9E). In conclusion, RBP4 may regulate the proliferation, invasion and migration of GC through the RAS/RAF/ERK axis. Finally, we made a mechanism map based on the relevant molecules involved in the regulation of RBP4 in this study (Figure 10).

Discussion

Gastric cancer (GC) is a highly heterogeneous disease that is molecularly complex and characterized by a myriad of interactions among genetic, environmental, and host factors. Over the past few years, advancements in biomedicine have led to significant progress in treating advanced GC and metastatic GC through molecular targeted therapy. Therefore, identifying novel GC targets is crucial for the creation of innovative medications for clinical use. Our research discovered that the expression of RBP4 was upregulated in GC, which may promote the development of GC through the RAS/RAF/ERK axis, and suggests that RBP4 may be a biological target for GC.

RBP4 is a lipid transport protein with a protein molecular weight of 21 KD, a single polypeptide chain in humans comprising 201 amino acids and 3 disulfide bonds.[14,15] It has been found that RBP4 is mainly composed of an N-terminal helix, a C-terminal α-helix and a characteristic β-barrel core.[16] One of the β-barrel cores can specifically house a retinol molecule, making this hydrophobic vitamin soluble in an aqueous environment. Due to its properties, over 99% of RBP4 get absorbed again by the proximal renal tubules, rendering RBP4 a remarkably accurate marker of renal tubular dysfunction.[17] Notably, the lack of megalux specific to the kidney in mice resulted in a decrease in the excretion of retinol in urine and retinol in the liver, as well as causing a decrease in urinary RBP4 levels. This indicates a more intricate function of the kidney in the in vivo regulation of vitamin A analogs.[18] RBP4 acts as a transporter of retinol and is recognized as the sole binding protein in the circulation,[19] and changes in RBP4 have been associated with a range of human ailments, including vision impairments and ocular disease,[20] disturbances in glucose and lipid homeostasis,[21] and cardiovascular disease.[22] Moreover, RBP4 has been reported in a variety of cancers, such as there is RBP4 expression up-regulated in colorectal cancer,[23] and RBP4 modulates trophoblast cell proliferation and invasion via the PI3K/AKT pathway.[24] However, RBP4 has not been completely explained in GC.

This study used bioinformatics to obtain information on the expression of RBP4 in a variety of cancers, as well as on the distribution of immune infiltration and drug resistance. The TCGA database revealed an increase in RBP4 expression in GC. Additionally, through analysis on the Kaplan-Meier plotter website, it was found that elevated levels of RBP4 were strongly associated with unfavorable outcomes in GC patients, indicating its potential as a prognostic marker for patient survival. For this, we demonstrated that RBP4 is overexpressed in GC tissues and cells at both the level of RNA transcriptional and protein translation. EMT is a versatile and pleiotropic transformation in the phenotype of epithelial cells as they transition to a mesenchymal state.[25] This reaction occurs when cells are stimulated by signals in embryonic growth stages and in specific conditions such as cancer.[26,27] EMT is involved in the development of tumors, contributing to tumorigenesis, invasion and metastasis. Additionally, EMT is linked to immune system suppression within the tumor microenvironment, resulting in reduced responsiveness to immune checkpoint inhibitor therapies. The initial discovery of this study revealed that knocking down RBP4 resulted in the inactivation of N-cadherin, MMP2, MMP3, and MMP9, as well as an increase in E-cadherin levels. This indicates that RBP4 plays a role in promoting the migration and invasion of GC cells through its regulation of the EMT pathway.

Apoptosis, a regulatory mechanism for cell death found in animals, involves the release of cytochrome C from mitochondria. This release is controlled by a delicate balance between the proapoptotic and antiapoptotic proteins of the BCL2 family and the effector caspases.[28] Apoptosis culminates in caspase-6-induced rupture of the nuclear membrane, leading to the cleavage of numerous intracellular proteins and breakdown of genomic DNA into nucleosome structures.[29,30] The activation cascade of caspases downstream of the release of mitochondrial cytochrome C contributes to apoptosis through both intrinsic and extrinsic pathways. This process is identified by the permeabilization of the outer membrane of the mitochondria, known as MOMP. The intrinsic pathway is activated due to the disruption of internal cellular balance caused by DNA damage, whereas the extrinsic pathway is started by the stimulation of receptors on the cell surface. The activation of caspase-3 is triggered by MOMP and the release of cytochrome C,[31] which is considered to be the point of apoptotic cell death that is irreversible. During this process, proapoptotic proteins belonging to the BCL2 family, like BAX, facilitate the release of cytochrome C into the cytoplasm. Additionally, the moderation of apoptosis by cyclin-dependent kinases is accomplished through the transcriptional repression of sensitizers.[32–34] In particular, the transcription factor P53 is a trigger for DNA repair mechanisms and cell cycle arrest, along with serving as another proapoptotic factor. In our study, we found that knockdown of RBP4 activated proapoptotic proteins such as Caspase3, BAX, and P53, which effectively promoted apoptosis in GC cells.

The RAS pathway is critical for regulating the growth of normal cells and dysregulation of this signaling pathway usually arises during tumorigenesis.[35,36] Alterations in the constituent molecules of this pathway, specifically the RAS proteins, result in significant impacts in many cancers.[37,38] Extracellular-signal-regulated kinase (ERK) promotes cell proliferation and metastasis, especially through upstream activation of epidermal growth factor receptor (EGFR) and RAS small guanosine triphosphatase (GTPases).[39] In our experiments, we showed that the activities of ERK, RAS, and RAF were inhibited in cells after knocking down RBP4. ERK plays a vital role as a downstream element in the RAS/RAF/ERK signaling cascade. Upon phosphorylation, it relocates to the nucleus, resulting in alterations to gene expression.[40] Thus, our data suggest that silencing RBP4 can inhibit the growth of GC cells by suppressing the RAS/RAF/ERK axis.

In summary, we reported that RBP4, a novel oncogene in GC, may promote the proliferation of GC cells via the RAS/RAF/ERK axis. Our findings highlight the important role of RBP4 in GC growth and metastasis, providing new and important targets for molecular therapy.

Conclusion

RBP4 expression was upregulated in GC cells and tissues, and knockdown of RBP4 promoted apoptosis and inhibited proliferation, invasion and migration in GC cells. Knockdown of RB4 inhibited tumor proliferation in vivo. RBP4 may promote the growth of GC cells by regulating the RAS/RAF/ERK signaling pathway. This study provides promising therapeutic targets for GC patients.

Funding

Key Laboratory of Basic and Clinical Transformation of Digestive and Metabolic Diseases, Yangzhou, China (YZ2020159).

Disclosure

The authors report no conflicts of interest in this work.

References

1. Smyth EC, Nilsson M, Grabsch HI, van Grieken NCT, Lordick F. Gastric cancer. *Lancet*. 2020;396(10251):635–648. doi:10.1016/S0140-6736(20)31288-5
2. Sung H, Ferlay J, Siegel RL, et al. Global cancer statistics 2020: GLOBOCAN estimates of incidence and mortality worldwide for 36 cancers in 185 countries. *CA Cancer J Clin*. 2021;71(3):209–249. doi:10.3322/caac.21660
3. Bray F, Ferlay J, Soerjomataram I, Siegel RL, Torre LA, Jemal A. Global cancer statistics 2018: GLOBOCAN estimates of incidence and mortality worldwide for 36 cancers in 185 countries. *CA Cancer J Clin*. 2018;68(6):394–424. doi:10.3322/caac.21492
4. Guan WL, He Y, Xu RH. Gastric cancer treatment: recent progress and future perspectives. *J Hematol Oncol*. 2023;16(1):57. doi:10.1186/s13045-023-01451-3
5. Patel TH, Cecchini M. Targeted therapies in advanced gastric cancer. *Curr Treat Options Oncol*. 2020;21(9):70. doi:10.1007/s11864-020-00774-4
6. Steinhoff JS, Lass A, Schupp M. Biological functions of RBP4 and its relevance for human diseases. *Front Physiol*. 2021;12:659977. doi:10.3389/fphys.2021.659977
7. Raghu P, Sivakumar B. Interactions amongst plasma retinol-binding protein, transthyretin and their ligands: implications in vitamin A homeostasis and transthyretin amyloidosis. *Biochim Biophys Acta*. 2004;1703(1):1–9. doi:10.1016/j.bbapap.2004.09.023
8. Kawaguchi R, Zhong M, Kassai M, Ter-Stepanian M, Sun H. STRA6-catalyzed vitamin A influx, efflux, and exchange. *J Membr Biol*. 2012;245(11):731–745. doi:10.1007/s00232-012-9463-1
9. Quadro L, Blaner WS, Salchow DJ, et al. Impaired retinal function and vitamin A availability in mice lacking retinol-binding protein. *EMBO j*. 1999;18(17):4633–4644. doi:10.1093/emboj/18.17.4633
10. Wang Y, Wang Y, Zhang Z. Adipokine RBP4 drives ovarian cancer cell migration. *J Ovarian Res*. 2018;11(1):29. doi:10.1186/s13048-018-0397-9
11. Wang DD, Zhao YM, Wang L, et al. Preoperative serum retinol-binding protein 4 is associated with the prognosis of patients with hepatocellular carcinoma after curative resection. *J Cancer Res Clin Oncol*. 2011;137(4):651–658. doi:10.1007/s00432-010-0927-3
12. Li M, Xu D, Xia X, et al. Sema3C promotes hepatic metastasis and predicts poor prognosis in gastric adenocarcinoma. *J Int Med Res*. 2021;49(4):3000605211009802. doi:10.1177/03000605211009802
13. Yang J, Weinberg RA. Epithelial-mesenchymal transition: at the crossroads of development and tumor metastasis. *Dev Cell*. 2008;14(6):818–829. doi:10.1016/j.devcel.2008.05.009
14. Rask L, Anundi H, Böhme J, et al. The retinol-binding protein. *Scand J Clin Lab Invest Suppl*. 1980;154:45–61.
15. Rask L, Anundi H, Fohlman J, Peterson PA. The complete amino acid sequence of human serum retinol-binding protein. *Ups J Med Sci*. 1987;92(2):115–146. doi:10.3109/03009738709178685
16. Newcomer ME, Jones TA, Aqvist J, et al. The three-dimensional structure of retinol-binding protein. *EMBO j*. 1984;3(7):1451–1454. doi:10.1002/j.1460-2075.1984.tb01995.x
17. Bonventre JV, Vaidya VS, Schmouder R, Feig P, Dieterle F. Next-generation biomarkers for detecting kidney toxicity. *Nat Biotechnol*. 2010;28(5):436–440. doi:10.1038/nbt0510-436
18. Raila J, Willnow TE, Schweigert FJ. Megalin-mediated reuptake of retinol in the kidneys of mice is essential for vitamin A homeostasis. *J Nutr*. 2005;135(11):2512–2516. doi:10.1093/jn/135.11.2512
19. Kanai M, Raz A, Goodman DS. Retinol-binding protein: the transport protein for vitamin A in human plasma. *J Clin Invest*. 1968;47(9):2025–2044. doi:10.1172/JCI105889
20. Li ZZ, Lu XZ, Liu JB, Chen L. Serum retinol-binding protein 4 levels in patients with diabetic retinopathy. *J Int Med Res*. 2010;38(1):95–99. doi:10.1177/147323001003800111
21. Yang Q, Graham TE, Mody N, et al. Serum retinol binding protein 4 contributes to insulin resistance in obesity and type 2 diabetes. *Nature*. 2005;436(7049):356–362. doi:10.1038/nature03711
22. Sun Q, Kiernan UA, Shi L, et al. Plasma retinol-binding protein 4 (RBP4) levels and risk of coronary heart disease: a prospective analysis among women in the nurses' health study. *Circulation*. 2013;127(19):1938–1947. doi:10.1161/CIRCULATIONAHA.113.002073

23. Abola MV, Thompson CL, Chen Z, et al. Serum levels of retinol-binding protein 4 and risk of colon adenoma. *Endocr Relat Cancer*. 2015;22(2):L1–4. doi:10.1530/ERC-14-0429
24. Li H, Cao G, Zhang N, et al. RBP4 regulates trophoblastic cell proliferation and invasion via the PI3K/AKT signaling pathway. *Mol Med Rep*. 2018;18(3):2873–2879. doi:10.3892/mmr.2018.9240
25. Taki M, Abiko K, Ukita M, et al. Tumor immune microenvironment during epithelial-mesenchymal transition. *Clin Cancer Res*. 2021;27(17):4669–4679. doi:10.1158/1078-0432.CCR-20-4459
26. Nieto MA, Huang RY, Jackson RA, Thiery JP. EMT: 2016. *Cell*. 2016;166(1):21–45. doi:10.1016/j.cell.2016.06.028
27. Yang J, Antin P, Berx G, et al. Guidelines and definitions for research on epithelial-mesenchymal transition. *Nat Rev Mol Cell Biol*. 2020;21(6):341–352. doi:10.1038/s41580-020-0237-9
28. Bertheloot D, Latz E, Franklin BS. Necroptosis, pyroptosis and apoptosis: an intricate game of cell death. *Cell Mol Immunol*. 2021;18(5):1106–1121.
29. Nicholson DW, Thornberry NA. Caspases: killer proteases. *Trends Biochem Sci*. 1997;22(8):299–306. doi:10.1016/S0968-0004(97)01085-2
30. Fraser A, Evan G. A license to kill. *Cell*. 1996;85(6):781–784. doi:10.1016/S0092-8674(00)81005-3
31. Liu X, Kim CN, Yang J, Jemmerson R, Wang X. Induction of apoptotic program in cell-free extracts: requirement for dATP and cytochrome c. *Cell*. 1996;86(1):147–157. doi:10.1016/S0092-8674(00)80085-9
32. Nakano K, Vousden KH. PUMA, a novel proapoptotic gene, is induced by p53. *Mol Cell*. 2001;7(3):683–694. doi:10.1016/S1097-2765(01)00214-3
33. Gojo I, Zhang B, Fenton RG. The cyclin-dependent kinase inhibitor flavopiridol induces apoptosis in multiple myeloma cells through transcriptional repression and down-regulation of Mcl-1. *Clin Cancer Res*. 2002;8(11):3527–3538.
34. Chen S, Dai Y, Pei XY, et al. CDK inhibitors upregulate BH3-only proteins to sensitize human myeloma cells to BH3 mimetic therapies. *Cancer Res*. 2012;72(16):4225–4237. doi:10.1158/0008-5472.CAN-12-1118
35. Barbacid M. ras genes. *Annu Rev Biochem*. 1987;56:779–827. doi:10.1146/annurev.bi.56.070187.004023
36. Cargnello M, Roux PP. Activation and function of the MAPKs and their substrates, the MAPK-activated protein kinases. *Microbiol Mol Biol Rev*. 2011;75(1):50–83. doi:10.1128/MMBR.00031-10
37. Gimple RC, Wang X. RAS: striking at the core of the oncogenic circuitry. *Front Oncol*. 2019;9:965. doi:10.3389/fonc.2019.00965
38. Simanshu DK, Nissley DV, McCormick F. RAS proteins and their regulators in human disease. *Cell*. 2017;170(1):17–33. doi:10.1016/j.cell.2017.06.009
39. Roberts PJ, Der CJ. Targeting the Raf-MEK-ERK mitogen-activated protein kinase cascade for the treatment of cancer. *Oncogene*. 2007;26(22):3291–3310. doi:10.1038/sj.onc.1210422
40. Asati V, Mahapatra DK, Bharti SK. PI3K/Akt/mTOR and Ras/Raf/MEK/ERK signaling pathways inhibitors as anticancer agents: structural and pharmacological perspectives. *Eur J Med Chem*. 2016;109:314–341. doi:10.1016/j.ejmech.2016.01.012